

Binding affinity of *Escherichia coli* RNA polymerase- σ^{54} holoenzyme for the *glnAp2*, *nifH* and *nifL* promoters

Sabine K. Vogel, Alexandra Schulz and Karsten Rippe^{1,*}

Deutsches Krebsforschungszentrum, Biophysik der Makromoleküle (H0500), Im Neuenheimer Feld 280, D-69120 Heidelberg, Germany and ¹Deutsches Krebsforschungszentrum, Molekulare Genetik (H0700), Im Neuenheimer Feld 280 and Kirchhoff-Institut für Physik, Physik molekularbiologischer Prozesse, Universität Heidelberg, Schröderstraße 90, D-69120 Heidelberg, Germany

Received February 25, 2002; Revised and Accepted July 22, 2002

ABSTRACT

Escherichia coli RNA polymerase associated with the σ^{54} factor (RNAP- σ^{54}) is a holoenzyme form that transcribes a special class of promoters not recognized by the standard RNA polymerase- σ^{70} complex. Promoters for RNAP- σ^{54} vary in their overall 'strength' and show differences in their response to the presence of DNA curvature between enhancer and promoter. In order to examine whether these effects are related to the promoter affinity, we have determined the equilibrium dissociation constant K_d for the binding of RNAP- σ^{54} to the three promoters *glnAp2*, *nifH* and *nifL*. Binding studies were conducted by monitoring the changes in fluorescence anisotropy upon titrating RNAP- σ^{54} to carboxy-rhodamine-labeled DNA duplexes. For the *glnAp2* and *nifH* promoters similar values of $K_d = 0.94 \pm 0.55$ nM and $K_d = 0.85 \pm 0.30$ nM were determined at physiological ionic strength, while the *nifL* promoter displayed a significantly weaker affinity with $K_d = 8.5 \pm 1.9$ nM. The logarithmic dependence of K_d on the ionic strength I was $-\Delta\log(K_d)/\Delta\log(I) = 6.1 \pm 0.5$ for the *glnAp2*, 5.2 ± 1.2 for the *nifH* and 2.1 ± 0.1 for the *nifL* promoter. This suggests that the polymerase can form fewer ion pairs with the *nifL* promoter, which would account for its weaker binding affinity.

INTRODUCTION

RNA polymerase from *Escherichia coli* complexed with the alternative σ factor σ^{54} (RNAP- σ^{54}) recognizes a specific class of promoters with conserved sequence elements around position -24 and -12 upstream of the transcription start site at +1 (1). RNAP- σ^{54} can bind to the promoter and form a stable closed complex. However, the enzyme is unable to melt the DNA at the transcription start site, i.e. to undergo the

transition into the open complex. This process involves specific transcription factors with ATPase activity as for example nitrogen regulatory protein C (NtrC or NR_{II}) or nitrogen fixation protein A (NifA). The binding sites of these proteins are located at upstream enhancer sequences and require looping of the DNA to enable interaction with RNAP- σ^{54} (2–6). The mechanism of transcription activation in this system has been discussed in recent reviews (7–9). Several lines of evidence indicate that the activator protein targets the σ^{54} subunit and works by triggering a conformational change that involves the N-terminus of σ^{54} (10).

In a number of studies differences in the relative strength of RNAP- σ^{54} promoters have been reported with respect to the *in vivo* RNA levels (11), the activity of a β -galactosidase reporter gene (12,13) or by measuring the equilibrium amount of open complexes formed *in vitro* in single round transcription experiments (14–16). Here we define the overall promoter strength as the rate with which the open complex RP_o of RNAP- σ^{54} (R) at a given promoter P is formed in a multi-step reaction according to equation 1.



In this equation 1 the forward and backward rate constants for the formation/dissociation of the closed complex RP_c are given by k_1 and k_{-1} so that the equilibrium dissociation constant $K_d = k_{-1}/k_1$ in equation 2 reflects the affinity of the promoter for RNAP- σ^{54} .

$$K_d = k_{-1}/k_1 = ([R] \cdot [P])/[RP_c] \quad 2$$

For the standard *E. coli* RNAP- σ^{70} holoenzyme a number of promoters have been analyzed in detail. It has been demonstrated that both the binding of the RNA polymerase to the promoter as well as the subsequent conversion of the closed complex into the open complex RP_o can be rate limiting (17). For RNAP- σ^{54} no quantitative analysis of the promoter strength in terms of the relative contributions of the separate

*To whom correspondence should be addressed. Tel: +49 6221 424620; Fax: +49 6221 42524676; Email: karsten.rippe@dkfz.de

Present address:

Alexandra Schulz, Roche Diagnostics, Sandhoferstraße 116, D-68305 Mannheim, Germany

steps has been reported so far. From footprinting experiments a K_d of 3 nM at approximately physiological salt concentrations was estimated for the *glnAp2* promoter (18). In contrast, the *nifH* (19,20) and *nifL* (21–23) promoters from *Klebsiella pneumoniae* showed no or only a very weak footprint under similar conditions. Accordingly, *glnAp2* has been designated as a 'strong' promoter as opposed to the 'weak' *nifH* and *nifL* promoters. However, it should be noted that both *glnAp2* and *nifH* are 'strong' promoters in the sense that they can be expressed at high levels under suitable physiological conditions (13,24). In contrast, the *nifL* promoter displayed an approximately 5-fold lower expression level than the *nifH* promoter (13). Here we have measured the equilibrium dissociation constant K_d dependence on the ionic strength for oligonucleotide duplexes with sequences from the *glnAp2*, *nifH* and *nifL* promoters. The binding of RNAP- σ^{54} to DNA was monitored by fluorescence anisotropy measurements using DNA oligonucleotide duplexes with a carboxyrhodamine end label.

MATERIALS AND METHODS

DNA and RNAP- σ^{54} preparation

HPLC-purified DNA oligonucleotides were purchased from PE-Applied Biosystems (Weiterstadt, Germany). The fluorescent dye 6-carboxy-X-rhodamine (ROX) was covalently attached to the 5'-end via a C6 linker. The extinction coefficients of the single DNA strands were determined as described previously (25). Equimolar amounts of complementary single strands were mixed in a buffer containing 10 mM Tris-HCl, pH 7.5, 10 mM NaCl, 0.1 mM EDTA and annealed by 2 min heating at 70°C followed by slow cooling to room temperature over several hours. Purification of the resulting DNA duplexes was done by extraction from native polyacrylamide gels according to Rippe *et al.* (26). From an analysis of various ROX-labeled DNAs of different lengths an average extinction coefficient of ROX attached to DNA of $\epsilon_{583} = 96\,000\text{ M}^{-1}\text{ cm}^{-1}$ at 25°C was calculated (J.F. Kepert and K. Rippe, unpublished results). This value was used to determine the concentration of the purified ROX-labeled DNA duplex stock solutions. The concentration of the unlabeled promoter duplexes was determined based on an extinction coefficient of $\epsilon_{260} = 559\,000\text{ M}^{-1}\text{ cm}^{-1}$ at 25°C. The sequences of the three ROX-labeled duplexes correspond to the *glnAp2* promoter from *E. coli* and to the *nifH* and *nifL* promoters from *K. pneumoniae* (Fig. 1) (1). In the *nifH* and *nifL* promoters the 5 bp found adjacent to the ROX label were kept identical to the *glnAp2* sequence in order to avoid differences in the spectroscopic properties of the ROX label.

RNA polymerase core enzyme from *E. coli* was purchased from Epicentre Technologies (Madison, WI). It was mixed with σ^{54} in a ratio of 1:1.5 to form the RNAP- σ^{54} holoenzyme at a stock concentration of $\sim 1\ \mu\text{M}$. This preparation was stored at -20°C in a buffer with 50 mM Tris-HCl, pH 7.5, 250 mM NaCl, 0.1 mM EDTA, 1 mM DTT and 50% glycerol. The σ^{54} protein does not bind to the wild-type *nifH* and *glnAp2* promoters in the absence of the core RNA polymerase (27,28). Only for a special mutant form of the *nifH* promoter (–17 to –15 sequence TTT) has binding of isolated σ^{54} ($K_d \approx 10^{-7}\text{ M}$) at moderate ionic strength been demonstrated (27). Thus, the

presence of excess σ^{54} protein should not affect the association of RNAP- σ^{54} with the sequences studied here.

The activity of the purified DNA duplexes and the RNAP- σ^{54} holoenzyme was confirmed in native gel electrophoresis. The purified DNA duplexes and ROX-labeled single strands were analyzed on a 20% native polyacrylamide gel. For the gel mobility shift assay 245 nM of the respective promoter DNA duplexes in $0.5\times$ RNAP- σ^{54} storage buffer were mixed with varying amounts of RNAP- σ^{54} holoenzyme. Complexes and free DNA were separated on a 5% polyacrylamide gel (29:1) and visualized by ethidium bromide staining.

Fluorescence anisotropy measurements

Fluorescence anisotropy measurements were performed with a SLM 8100 fluorescence spectrometer (SLM Aminco Inc.) using an L-format setup. The ROX excitation wavelength of 580 nm was selected with a double grating monochromator using an 8 or 16 nm slit width for high intensity. In the emission channel scattered light was suppressed with a 610 nm cut-off filter. Intensity variations of the lamp were corrected by normalization to a reference channel with a rhodamine quantum counter. All measurements were conducted at 25°C in a buffer containing 20 mM HEPES-KOH, pH 8.0, 5 mM magnesium acetate, 1 mM DTT, 0.1 mg/ml BSA, 0.01% NP-40 detergent (Roche Diagnostics, Germany), supplemented with potassium acetate at a concentration from 50 to 350 mM.

According to the Perrin equation (29), the anisotropy of a fluorescent complex increases with its volume and reflects its rotational mobility. The assay used here is based on the rationale that the free DNA has a relatively low fluorescence anisotropy. This signal increases upon protein binding, due to the reduced rotational diffusion time after formation of the protein-DNA complex. The same approach has been used successfully in a number of studies (see for example 25,30–35).

The RNAP- σ^{54} DNA binding activity was determined by stoichiometric titrations at a DNA concentration of 10 nM duplex in low salt binding buffer (50 mM potassium acetate) for high affinity binding. From the linear increase at low protein concentration and the plateau region obtained at saturation of the binding sites the equivalence point for the formation of a 1:1 complex was determined. In these experiments a DNA binding activity between 80 and 90% with respect to the core polymerase concentration given by the manufacturer was determined for different RNAP- σ^{54} holoenzyme preparations (data not shown).

For the determination of dissociation constants a DNA solution with 25–200 pM duplex in binding buffer was titrated with a RNAP- σ^{54} protein solution diluted into the same buffer. After addition of protein the sample was equilibrated for ~ 3 min before measuring the equilibrium anisotropy value. For each anisotropy value the average of 20 measurements with an integration time of 5 s was determined. To check whether the quantum yield of the ROX dye changed upon binding of the polymerase the fluorescence intensity of the free promoter DNA and the intensity after saturation of the DNA binding sites was recorded under polarization-independent 'magic angle' conditions (vertically polarized excitation and emission polarizer oriented at 54.7°) for every titration.

Data analysis

Equilibrium binding data were analyzed according to the reaction given in equation 1 for the formation of a 1:1 complex between RNAP· σ^{54} and the ROX-labeled duplex with the promoter sequence. The DNA duplex concentration $[P]$ in the experiments was chosen so that $10 \cdot [P] \leq K_d$. Under these conditions the concentration of free RNAP· σ^{54} $[R]$ can be approximated by the total polymerase concentration $[R_{tot}]$, i.e. $[R] \approx [R_{tot}]$, and the fractional saturation θ of the promoter duplex with RNAP· σ^{54} is given by

$$\theta = [R_{tot}] / ([R_{tot}] + K_d) = (r - r_P) / (r_{RP} - r_P) \quad 3$$

In equation 3 r is the measured anisotropy at a given polymerase concentration. The anisotropy values of the free promoter DNA and that of the RP_c complex are given by r_P and r_{RP} , respectively. Rearrangement of equation 3 leads to equation 4, which was used to determine K_d from a least squares fit of the binding curve obtained by plotting r versus the added RNA polymerase concentration $[R_{tot}]$ with r_P and r_{RP} as additional fit parameters.

$$r = (r_P \cdot K_d + [R_{tot}] \cdot r_{RP}) / ([R_{tot}] + K_d) \quad 4$$

The least squares fit was computed with the program Kaleidagraph v.3.5 (Synergy Software, PA). The use of equation 4 is only correct if the quantum yield of the ROX dye does not change upon binding of RNAP· σ^{54} , which was the case in the experiments reported here (see below).

RESULTS

Gel analysis of ROX-labeled promoter DNA

The oligonucleotide duplexes of 43 bp length shown in Figure 1 were studied with respect to their binding affinity for RNAP· σ^{54} . The sequences correspond to the *glnAp2* promoter from *E.coli* and the *nifH* and *nifL* promoters from *K.pneumoniae*. All duplexes carried the fluorescent dye ROX at the 5'-end. Gel analysis of the purified duplexes is shown in Figure 2A (three left lanes) in comparison to the ROX-labeled single strands (Fig. 2A, three right lanes), which displayed a higher electrophoretic mobility. Both the ROX fluorescence signal as well as ethidium bromide staining of the duplexes revealed only a single band demonstrating that the synthesis and reconstitution of the promoter DNA sequences was successful.

The binding of RNAP· σ^{54} to these duplexes was qualitatively characterized in an electrophoretic gel mobility shift assay under conditions of stoichiometric binding (Fig. 2B). Both the RNAP· σ^{54} enzyme and the DNA promoter sequences were active with respect to binding as indicated by the almost fully shifted DNA fraction at an approximate 1:1 ratio of protein and DNA (Fig. 2B, highest protein concentrations).

Binding affinity of RNAP· σ^{54} for *glnAp2*, *nifH* and *nifL* promoters

In order to measure the dissociation constant K_d of RNAP· σ^{54} with the three different promoters under true equilibrium conditions and at defined ionic strength and pH the binding of RNAP· σ^{54} was followed by fluorescence anisotropy

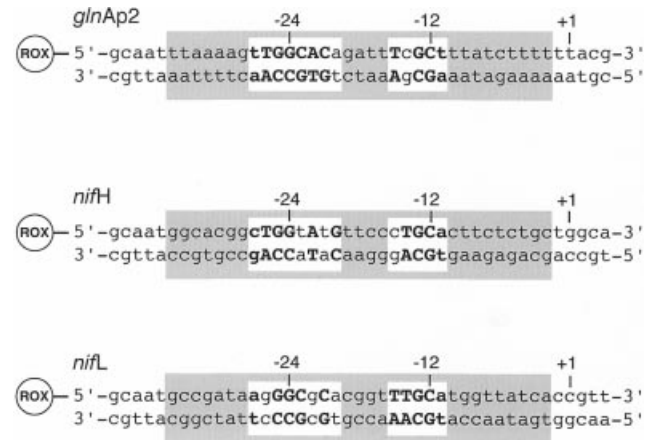


Figure 1. Three different ROX-labeled DNA duplexes were used in the binding studies, the *glnAp2* promoter sequence from *E.coli* and the *nifH* and *nifL* promoters from *K.pneumoniae*. The nucleotides that fit the -24/-12 consensus sequence for RNAP· σ^{54} -specific promoters are in bold (1). The RNAP binding region from about -34 close to the transcription start site at position -2 is shaded in gray and has been derived from footprinting studies (44,45). Positions +1, -12 and -24 relative to the RNA transcript start site are indicated.

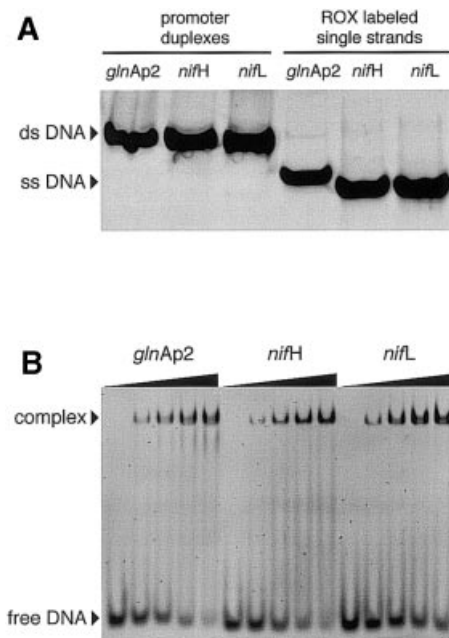


Figure 2. Gel electrophoretic analysis of ROX-labeled promoter duplexes and RNAP· σ^{54} -DNA complexes. (A) Native polyacrylamide gel of promoter duplexes (three left lanes) and ROX-labeled single strands (three right lanes). (B) Gel shift analysis of RNAP· σ^{54} complexes with the three promoter DNA duplexes. The five lanes for each promoter sequence display an increasing ratio of RNAP· σ^{54} to the DNA duplex (245 nM concentration) from 0:1, 0.25:1, 0.5:1, 0.75:1 to 1:1.

measurements. The polymerase was titrated into a solution of the ROX-labeled DNA duplex at a given salt concentration. Protein was added until all binding sites were saturated and the anisotropy reached a plateau value, which reflects the anisotropy of the 1:1 complex of RNAP· σ^{54} with the DNA. The resulting binding curve was fitted to equation 4 and K_d as

Table 1. Fluorescence anisotropy parameters for the binding of RNAP- σ^{54} to the *glnAp2*, *nifH* and *nifL* promoters

| | <i>glnAp2</i> | <i>nifH</i> | <i>nifL</i> |
|---|---------------|--------------|--------------|
| Anisotropy of free DNA (r_P) ^a | 0.165 ± 0.02 | 0.169 ± 0.01 | 0.166 ± 0.01 |
| Anisotropy of complex (r_{RP}) ^a | 0.244 ± 0.03 | 0.260 ± 0.01 | 0.266 ± 0.02 |
| Quenching factor q ^b | 1.13 ± 0.1 | 1.08 ± 0.1 | 1.0 ± 0.1 |

^aThe anisotropies of free (r_P) and complexed DNA (r_{RP}) were derived from fitting the binding curves to equation 4.

^bThe quenching factor q was determined for every titration under polarization-independent conditions and averaged.

well as the anisotropies of the free promoter DNA (r_P) and the protein–DNA complex (r_{RP}) were obtained. As expected, similar average values of both r_P (0.165–0.169) and r_{RP} (0.244–0.266) were obtained for the three promoters indicating similar rotational diffusion times for the free DNA and its complex with the polymerase (Table 1).

The analysis of the binding curve according to equation 4 is only valid if the quantum yield of the ROX dye does not change upon binding of the polymerase (36). To test whether this was the case the fluorescence intensities of each sample before and after the titration were measured. After correction for dilution these intensity ratios corresponded to quenching factors q of 1.13 ± 0.1 (*glnAp2*), 1.08 ± 0.1 (*nifH*) and 1.02 ± 0.1 (*nifL*) (Table 1). Thus, within the accuracy of the measurements, the binding of RNAP- σ^{54} to the promoter DNA did not change the ROX quantum yield so that the analysis of the data according to equation 4 is valid.

Figure 3 displays representative binding curves recorded by titrating the *glnAp2*, *nifH* and *nifL* promoters at an approximately physiological ionic strength (200 mM potassium acetate and 5 mM magnesium acetate, $I = 0.229$ M). The data were fitted to equation 4 to obtain K_d , r_P and r_{RP} (Fig. 3A). The measured r values were then converted according to equation 3 into the fractional saturation of the DNA θ (Fig. 3B). A good agreement of the measured data according to the 1:1 binding model described by equations 3 and 4 was obtained yielding K_d values of 0.7 ± 0.1 (*glnAp2*), 1.2 ± 0.1 (*nifH*) and 10.1 ± 1.1 nM (*nifL*) for the titrations shown in Figure 3. While the *glnAp2* and *nifH* promoters displayed a similar affinity at an ionic strength of $I = 0.229$ M, binding to the *nifL* sequence was about an order of magnitude weaker. Average values from multiple measurements are summarized in Table 2 with K_d values of 0.94 ± 0.55 (*glnAp2*), 0.85 ± 0.30 (*nifH*) and 8.5 ± 1.9 nM (*nifL*) at $I = 0.229$ M.

In addition, whether the ROX-fluorophore affected the differences in binding affinities observed in the experiments described above was tested at the same ionic strength with unlabeled DNA duplexes. A 10 nM solution of preformed RNAP- σ^{54} complex with a given ROX-labeled promoter DNA was titrated with unlabeled *glnAp2*, *nifH* or *nifL* duplex. The concentration of the unlabeled DNA which was required to displace 50% of the ROX–DNA from the complex with RNAP- σ^{54} was determined. For titrating *glnAp2*–ROX with *nifH* and *nifH*–ROX with *glnAp2* this concentration was the same within ~10%. Thus, the unlabeled *glnAp2* and *nifH* promoter fragments displayed essentially the same binding affinities at physiological ionic strength. In contrast, the *nifL* promoter (*nifL*–ROX versus *glnAp2*, *nifL*–ROX versus *nifH* and

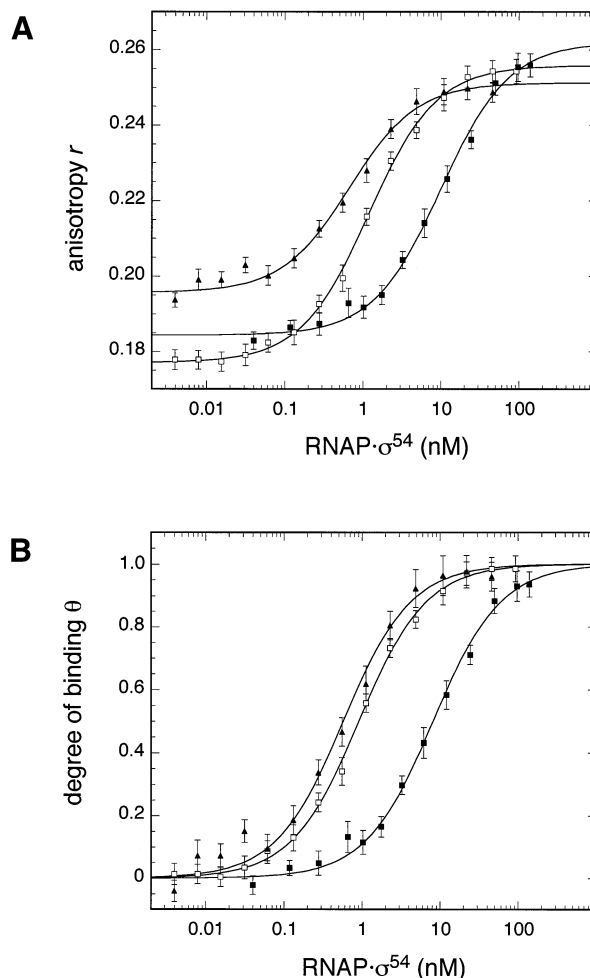


Figure 3. Fluorescence anisotropy measurement of RNAP- σ^{54} binding to different promoter sequences. A comparison of the binding affinity to three promoter duplexes at approximately physiological ionic strength is shown. The ROX-labeled DNA at a concentration of 50 pM for *glnAp2* (filled triangles) and *nifH* (open squares) and of 100 pM for *nifL* (filled squares) was preincubated in a buffer supplemented with 200 mM potassium acetate and 5 mM magnesium acetate ($I = 0.229$ M). This solution was titrated with the indicated concentrations of RNAP- σ^{54} . (A) The resulting binding curves of anisotropy r versus RNAP- σ^{54} concentration were analyzed according to equation 4 to determine K_d . Values of 0.7 ± 0.1 (*glnAp2*), 1.2 ± 0.1 (*nifH*) and 10.1 ± 1.1 nM (*nifL*) were obtained for the experiments shown in this figure. Average K_d values at various salt concentrations are given in Table 2. (B) To account for differences in the values of r_P and r_{RP} between the three promoters the measured anisotropy values can be converted into the fractional saturation of the DNA θ according to equation 3 for a direct comparison of the titrations.

glnAp2–ROX versus *nifL*) displayed a significantly weaker association with RNAP- σ^{54} .

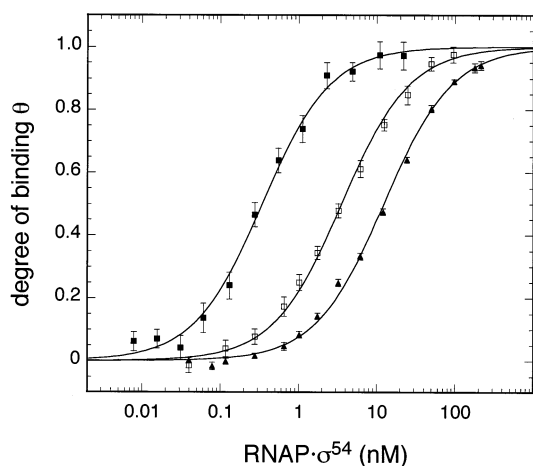
Salt dependence of RNAP- σ^{54} promoter binding affinity

When the experiments were performed at different salt concentrations in the range $I = 0.079$ – 0.379 M K^+ equivalents the value of K_d increased at higher ionic strength. This is due to a weakening of electrostatic interactions between protein and DNA as reviewed in Record *et al.* (37). An example of this type of experiment is given in Figure 4, which shows binding curves of the *nifL* promoter in buffer supplemented with

Table 2. Dissociation constants K_d for the binding of RNAP- σ^{54} to the *glnAp2*, *nifH* and *nifL* promoters as determined by fluorescence anisotropy measurements

| Salt concentration | K_d (nM) <i>glnAp2</i> | K_d (nM) <i>nifH</i> | K_d (nM) <i>nifL</i> |
|--|--------------------------|------------------------|------------------------|
| 50 mM potassium acetate $I = 0.079$ M | | | 0.76 ± 0.56 (5) |
| 100 mM potassium acetate $I = 0.129$ M | | | 3.2 ± 1.7 (4) |
| 150 mM potassium acetate $I = 0.179$ M | 0.40 ± 0.04 (4) | 0.50 ± 0.36 (3) | 4.6 ± 0.9 (2) |
| 200 mM potassium acetate $I = 0.229$ M | 0.94 ± 0.55 (6) | 0.85 ± 0.30 (3) | 8.5 ± 1.9 (3) |
| 250 mM potassium acetate $I = 0.279$ M | 5.1 ± 2.3 (13) | 2.4 ± 0.7 (4) | 10 ± 8 (7) |
| 300 mM potassium acetate $I = 0.329$ M | 11 ± 9 (6) | 16 ± 10 (3) | 18 ± 13 (3) |
| 350 mM potassium acetate $I = 0.379$ M | 15 ± 11 (8) | 40 ± 11 (3) | |

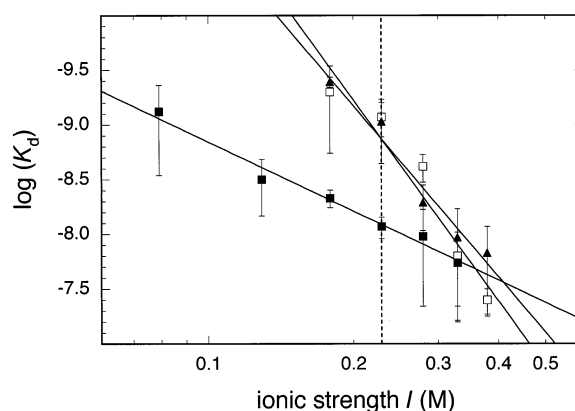
Average values for K_d and corresponding standard deviations are given in nanomolar concentrations and were determined in binding buffer (20 mM HEPES-KOH, pH 8.0, 5 mM magnesium acetate, 1 mM DTT, 0.1 mg/ml BSA, 0.01% NP-40), supplemented with the indicated potassium acetate concentrations, yielding the indicated ionic strength I . The number in parentheses after the value of the dissociation constant refers to the number of experiments averaged.

**Figure 4.** Representative binding curves of *nifL* at different ionic strength. Data are shown for 50 mM (filled squares), 150 mM (open squares) and 250 mM (filled triangles) potassium acetate buffer. The concentration of DNA in the given buffer was 25 pM for the 50 mM potassium acetate buffer and 200 pM for the higher salt concentrations.

potassium acetate at a concentration of 50 mM ($K_d = 0.43$ nM), 150 mM ($K_d = 5.2$ nM) and 250 mM ($K_d = 22$ nM). A plot of the logarithm of the average K_d values determined at a given salt concentration versus the logarithm of the ionic strength displayed an apparently linear relation (Fig. 5). The slopes of this plot $-\Delta \log(K_d)/\Delta \log(I)$ were 6.1 ± 0.5 (*glnAp2*), 5.2 ± 1.2 (*nifH*) and 2.1 ± 0.1 (*nifL*). This means that the dissociation constant became weaker by a factor of $10^{6.1}$ (*glnAp2*), $10^{5.2}$ (*nifH*) and $10^{2.1}$ (*nifL*) per decade of higher ionic strength. Again, the *glnAp2* and *nifH* promoters were indistinguishable within the accuracy of the measurements, whereas the *nifL* promoter showed a much weaker salt dependence.

DISCUSSION

The promoter binding affinity of RNAP- σ^{54} as expressed by the dissociation constant K_d is an important parameter for analyzing the strength of different promoters. In addition, other steps involved in the activation pathway leading to the melting of the DNA at the transcription start site (open complex formation) could also be rate limiting (equations 1

**Figure 5.** Effect of ionic strength on binding affinity. All K_d values for the *glnAp2* (filled triangles), *nifH* (open squares) and *nifL* (filled squares) promoters are displayed in a double-logarithmic plot against the ionic strength I (see Table 1). The lines correspond to linear regressions according to $\log(K_d) = -5.6 + 5.2 \log(I)$ (*glnAp2*), $\log(K_d) = -5.0 + 6.1 \log(I)$ (*nifH*) and $\log(K_d) = -6.8 + 2.1 \log(I)$ (*nifL*).

and 2). These involve the interaction of the closed complex with the activator protein at the enhancer, the release of the block imposed by σ^{54} to open complex formation as well as the kinetics of the isomerization step itself. Here we report data for the binding affinity of RNAP- σ^{54} to the *E. coli glnAp2* promoter and the two promoters *nifH* and *nifL* from *K. pneumoniae* (Fig. 1). Promoters for RNAP- σ^{54} are characterized by the -24 consensus sequence 5'-(T/C)TGGCACG-3' (-27 to -20) and a conserved 5'-TTGC(A/T)-3' (-15 to -11) at position -12 (1). All three promoters have conserved -25/-24 and -13/-12 residues, changes of which have been shown to strongly reduce binding of RNAP- σ^{54} (11,27). The *glnAp2* promoter most closely resembles the above consensus sequence (two deviations at -20 and at -14) whereas *nifH* (-23, -21 and -15) and *nifL* (-26, -22 and -20) have differences in three positions. A change of the G-C base pair at position -22 in the *nifL* sequence into the consensus A-T increased the expression level more than 2-fold (38). However, the simple assumption that the consensus sequence with conserved residues from -27 to -20 and -15 to -11 provides the highest rate of transcription initiation appears not

to be correct, as deduced from an *in vivo* comparison of 17 promoter sequences (11). In this context it is noteworthy that the *glnAp2* promoter has a consecutive tract of seven A·T base pairs from -5 to +2 whereas for the *nifH* and *nifL* promoter only two or three A·T base pairs are found in this region (Fig. 1). This might lead to differences in the kinetics of strand separation during open complex formation.

It has been shown for RNAP· σ^{70} holoenzyme that the promoter affinity is strongly dependent on the ionic strength (39,40). Accordingly, the K_d for RNAP· σ^{54} was quantitated at different salt concentrations. The ionic strength in *E. coli* varies between 0.17 and 0.3 M K^+ equivalents (41,42) and an *in vivo* activity of divalent cations such as Mg^{2+} between 1 and 10 mM has been estimated (43). Since Mg^{2+} is also essential for the synthesis activity of RNA polymerase it was included at a concentration of 5 mM in all fluorescence anisotropy binding measurements. Typical physiological conditions should correspond to an ionic strength around $I = 0.23$ M, which is indicated in Figure 5. At this ionic strength average K_d values of 0.94 ± 0.55 and 0.85 ± 0.3 nM for the *nifH* and *glnAp2* promoters and 8.5 ± 1.9 nM for the *nifL* promoter were measured (Table 2). Thus, the *nifL* promoter displayed an about 10-fold lower binding affinity as compared to the two other promoters. The results for the *glnAp2* and *nifL* promoters are in good agreement with previous footprinting experiments (18,21–23). However, the *nifH* promoter showed an unexpectedly high affinity under these conditions very similar to that of *glnAp2* (Table 2). This is in contrast to the footprinting data, which revealed a much lower occupancy of the *nifH* promoter as compared to the *glnAp2* promoter (19,20). Furthermore, a mutation of the CCC residues in the *nifH* promoter from -15 to -17 to TTT as in the *glnAp2* sequence (Fig. 1) increased the footprinting protection (19). Mutations of C to T at -15 and -16 enhanced integration host factor (IHF)-independent gene expression in an *in vitro* transcription/translation assay (12) indicating that the binding affinity is also related to the promoter strength. In the fluorescence anisotropy binding experiments described here the *glnAp2* and *nifH* promoters showed comparable K_d values over the whole range of salt concentrations whereas the *nifL* promoter displayed a much weaker salt dependence. This excludes the possibility that the apparently very similar binding affinities of the *glnAp2* and *nifH* promoters is restricted to a certain ionic strength, and it is unclear how the differences between our results and those of the footprinting experiments described in Morret and Buck (19) and Buck and Cannon (20) can be explained. The determination of binding affinities by monitoring changes in the fluorescence anisotropy of dye-labeled DNA duplexes as it has been used here is a true equilibrium method. It is applicable for accurate determinations of K_d values over a large range of solution conditions (25,30–35). A potential source of errors could be an effect of the fluorescent dye on the binding affinity as compared to the unlabeled DNA. For the present set of duplexes a spacer sequence of 5 bp (~17 Å length) separates the dye attached to a flexible alkyl linker of ~9 Å length from the RNAP· σ^{54} binding region as determined by footprinting (44,45). Accordingly, a direct interaction between dye and polymerase appears unlikely but cannot be excluded, since the high resolution structure of the RNAP· σ^{54} closed complex is presently unknown. However, when preformed complexes of the ROX-labeled promoters with

RNAP· σ^{54} were titrated with unlabeled *glnAp2* and *nifH* duplexes no significant differences in their affinities were observed. Thus, we infer that the dye label had no effect on the relative binding affinities. It is also conceivable that residues outside the region protected in the footprinting experiments affect the binding affinity. In addition, the apparent contradiction between the fluorescence anisotropy and footprinting analysis of binding to the *nifH* promoter could be explained by a different mode of binding to *nifH* as opposed to *glnAp2*, which could lead to a change in the protection pattern.

A characteristic feature of protein–nucleic acid interactions is the strong dependence of K_d on the ion concentration. The slope of the regression line $-\Delta\log(K_d)/\Delta\log(I)$ in the double logarithmic plot with $\log(K_d)$ versus the log of the salt concentration (Fig. 5) can be used to calculate the number of salt bridges between a protein and its DNA binding site in the absence of divalent ions (37,39,40,46,47). For the RNAP· σ^{70} closed complex at 0°C a value of 10.5 ± 1.5 has been determined with the T7 A1 promoter, which corresponds to about 12 salt bridges formed between polymerase and DNA (39). If Mg^{2+} is present in addition to monovalent ions, it acts as a competitor with the negatively charged phosphate groups of the DNA backbone. This leads to a reduction in the apparent slope and some curvature in the log-log plot, especially at higher Mg^{2+} concentrations (39,40). This effect is relevant for the binding studies described here, which were conducted in the presence of 5 mM $MgCl_2$. Since our data set did not display a significant curvature in the range of salt concentration studied the data were fitted with a linear regression line. Values of the slope of 6.1 ± 0.5 (*glnAp2*) and 5.2 ± 1.2 (*nifH*) were obtained (Table 1). From the data reported in Strauss *et al.* (39) and Shaner *et al.* (40) a value of $-\Delta\log(K_d)/\Delta\log(I) \approx 6$ in the range 0.1–0.4 M NaCl is estimated for RNAP· σ^{70} for a concentration of 5 mM Mg^{2+} . This suggests that similar numbers of salt bridges are formed in the closed complex of RNAP· σ^{54} with the *glnAp2* and *nifH* promoters as compared to the RNAP· σ^{70} T7 A1 promoter. In contrast, the slope of the salt dependence of the *nifL* promoter was clearly reduced and a value of 2.1 ± 0.1 was measured (Fig. 5 and Table 1). This demonstrates that the number of ion pairs between RNAP· σ^{54} and the *nifL* sequence is significantly smaller as compared to the two other promoters. We conclude that the reduced strength of the *nifL* promoter can be explained by its weak binding affinity due to a reduced number of electrostatic interactions with this promoter DNA.

Apart from overall strength, the three promoters for RNAP· σ^{54} are also different in their response to intrinsic DNA curvature and bending induced by binding of IHF. On the basis of the available data it appears that transcription activation of a ‘strong’ promoter like *glnAp2* by NtrC or NifA on superhelical templates is not facilitated by DNA curvature (48). In contrast, the *nifH* and *nifL* promoters showed a 3- to 20-fold increase in the equilibrium amount of open complexes in single round transcription experiments if a curved sequence or IHF-induced bending was present between enhancer and promoter (12,49–51). This observation can be explained by a model in which the strong *glnAp2* promoter has a higher affinity than the *nifH* and *nifL* promoters (48), which is supported by footprinting experiments (18–23). The K_d measurements reported here clearly demonstrate that the *glnAp2* promoter has a significantly higher binding affinity

than the *nifL* promoter. However, the differences in promoter occupation reported previously between the *glnAp2* and *nifH* promoters were not detected in our experiments, as discussed above. The about 20-fold stimulation of open complex formation by IHF or by an intrinsically curved DNA sequence at the *nifH* promoter on supercoiled DNA is not observed with the *glnAp2* promoter (12,48,49,51). If the two promoters indeed have very similar binding affinities for RNAP- σ^{54} other steps in the activation reaction that leads to open complex formation must be responsible for the observed differences with respect to promoter strength and the effect of DNA bending.

ACKNOWLEDGEMENTS

We acknowledge the support of Jörg Langowski. Part of the work by K.R. was done at the division Biophysik der Makromoleküle of the Deutsches Krebsforschungszentrum. The project was funded by the DFG (grant Ri 828-1) and by the Volkswagen Foundation in the program Junior Research Groups at German Universities.

REFERENCES

- Barrios,H., Valderrama,B. and Morett,E. (1999) Compilation and analysis of sigma(54)-dependent promoter sequences. *Nucleic Acids Res.*, **27**, 4305–4313.
- Wedel,A., Weiss,D.S., Popham,D., Dröge,P. and Kustu,S. (1990) A bacterial enhancer functions to tether a transcriptional activator near a promoter. *Science*, **248**, 486–490.
- Reitzer,L.J. and Magasanik,B. (1986) Transcription of *glnA* in *E. coli* is stimulated by activator bound to sites far from the promoter. *Cell*, **45**, 785–792.
- North,A.K., Klose,K.E., Stedman,K.M. and Kustu,S. (1993) Prokaryotic enhancer-binding proteins reflect eukaryote-like modularity: the puzzle of nitrogen regulatory protein C. *J. Bacteriol.*, **175**, 4267–4273.
- Collado-Vides,J., Magasanik,B. and Gralla,J.D. (1991) Control site location and transcriptional regulation in *Escherichia coli*. *Microbiol. Rev.*, **55**, 371–394.
- Rippe,K., Guthold,M., von Hippel,P.H. and Bustamante,C. (1997) Transcriptional activation via DNA-looping: visualization of intermediates in the activation pathway of *E. coli* RNA polymerase-sigma 54 holoenzyme by scanning force microscopy. *J. Mol. Biol.*, **270**, 125–138.
- Gralla,J.D. (2000) Signaling through sigma. *Nature Struct. Biol.*, **7**, 530–532.
- Buck,M., Gallegos,M.T., Studholme,D.J., Guo,Y. and Gralla,J.D. (2000) The bacterial enhancer-dependent sigma(54) (sigma(N)) transcription factor. *J. Bacteriol.*, **182**, 4129–4136.
- Xu,H. and Hoover,T.R. (2001) Transcriptional regulation at a distance in bacteria. *Curr. Opin. Microbiol.*, **4**, 138–144.
- Cannon,W.V., Gallegos,M.T. and Buck,M. (2000) Isomerization of a binary sigma-promoter DNA complex by transcription activators. *Nature Struct. Biol.*, **7**, 594–601.
- Wang,L. and Gralla,J.D. (1998) Multiple *in vivo* roles for the –12-region elements of sigma 54 promoters. *J. Bacteriol.*, **180**, 5626–5631.
- Hoover,T.R., Santero,E., Porter,S. and Kustu,S. (1990) The integration host factor stimulates interaction of RNA polymerase with NIFA, the transcriptional activator for nitrogen fixation operons. *Cell*, **63**, 11–22.
- Dixon,R., Eady,R.R., Espin,G., Hill,S., Iaccarino,M., Kahn,D. and Merrick,M. (1980) Analysis of regulation of *Klebsiella pneumoniae* nitrogen fixation (*nif*) gene cluster with gene fusions. *Nature*, **286**, 128–132.
- Carmona,M. and Magasanik,B. (1996) Activation of transcription of σ^{54} -dependent promoters on linear templates requires intrinsic or induced bending of the DNA. *J. Mol. Biol.*, **261**, 348–356.
- Carmona,M., Claverie-Martin,F. and Magasanik,B. (1997) DNA bending and the initiation of transcription at σ^{54} -dependent bacterial promoters. *Proc. Natl Acad. Sci. USA*, **94**, 9568–9572.
- Whitehall,S., Austin,S. and Dixon,R. (1992) DNA supercoiling response of the σ^{54} -dependent *Klebsiella pneumoniae nifL* promoter *in vitro*. *J. Mol. Biol.*, **225**, 591–607.
- McClure,W.R. (1980) Rate-limiting steps in RNA chain initiation. *Proc. Natl Acad. Sci. USA*, **77**, 5634–5638.
- Popham,D.L., Keener,J. and Kustu,S. (1991) Purification of the alternative σ factor, σ^{54} , from *Salmonella thyphimurium* and characterisation of σ^{54} -holoenzyme. *J. Biol. Chem.*, **266**, 19510–19518.
- Morret,E. and Buck,M. (1989) *In vivo* studies on the interaction of RNA polymerase- σ^{54} with the *Klebsiella pneumoniae* and *Rhizobium meliloti nifH* promoters. *J. Mol. Biol.*, **210**, 65–77.
- Buck,M. and Cannon,W. (1992) Activator-independent formation of a closed complex between σ^{54} -holoenzyme and *nifH* and *nifU* promoters of *Klebsiella pneumoniae*. *Mol. Microbiol.*, **6**, 1625–1630.
- Wong,P.K., Popham,D., Keener,J. and Kustu,S. (1987) *In vitro* transcription of the nitrogen fixation regulatory operon *nifLA* of *Klebsiella pneumoniae*. *J. Bacteriol.*, **169**, 2876–2880.
- Minchin,S.D., Austin,S. and Dixon,R.A. (1989) Transcriptional activation of the *Klebsiella pneumoniae nifLA* promoter by NTRC is face-of-the-helix dependent and the activator stabilizes the interaction of sigma 54-RNA polymerase with the promoter. *EMBO J.*, **8**, 3491–3499.
- Austin,S., Kundrot,C. and Dixon,R. (1991) Influence of a mutation in the putative nucleotide binding site of the nitrogen regulatory protein NTRC on its positive control function. *Nucleic Acids Res.*, **19**, 2281–2287.
- Weiss,D.S., Klose,K.E., Hoover,T.R., North,A.K., Porter,S.C., Wedel,A.B. and Kustu,S. (1992) Prokaryotic transcriptional enhancers. In McKnight,S.L. and Yamamoto,K.R. (eds), *Transcriptional Regulation*. Cold Spring Harbor Laboratory Press, Cold Spring Harbor, NY, Vol. 2, pp. 667–694.
- Sevenich,F.W., Langowski,J., Weiss,V. and Rippe,K. (1998) DNA binding and oligomerization of NtrC studied by fluorescence anisotropy and fluorescence correlation spectroscopy. *Nucleic Acids Res.*, **26**, 1373–1381.
- Rippe,K., Mücke,N. and Schulz,A. (1998) Association states of the transcription activator protein NtrC from *E. coli* determined by analytical ultracentrifugation. *J. Mol. Biol.*, **278**, 915–933.
- Buck,M. and Cannon,W. (1992) Specific binding of the transcription factor sigma-54 to promoter DNA. *Nature*, **358**, 422–424.
- Atkinson,M.R. and Ninfa,A.J. (1994) Mechanism and regulation of transcription from bacterial σ^{54} -dependent promoters. In Conaway,R.C. and Conaway,J.W. (eds), *Transcription: Mechanism and Regulation*. Raven Press, New York, NY, pp. 323–342.
- Perrin,F. (1926) Polarisation de la lumière de fluorescence. Vie moyenne des molécules dans l'état excité. *J. Phys. Radiat. V Ser. 6*, **7**, 390–401.
- Heyduk,T. and Lee,J.C. (1990) Application of fluorescence energy transfer and polarization to monitor *Escherichia coli* cAMP receptor protein and lac promoter interaction. *Proc. Natl Acad. Sci. USA*, **87**, 1744–1748.
- Heyduk,T., Lee,J.C., Ebright,Y.W., Blatter,E.E., Zhou,Y. and Ebright,R.H. (1993) CAP interacts with RNA polymerase in solution in the absence of promoter DNA. *Nature*, **364**, 548–549.
- LeTilly,V. and Royer,C.A. (1993) Fluorescence anisotropy assays implicate protein-protein interactions in regulating trp repressor DNA binding. *Biochemistry*, **32**, 7753–7758.
- Guest,C.R., Hochstrasser,R.A., Dupuy,C.G., Allen,D.J., Benkovic,S.J. and Millar,D.P. (1991) Interaction of DNA with the Klenow fragment of DNA polymerase I studied by time-resolved fluorescence spectroscopy. *Biochemistry*, **30**, 8759–8770.
- Reedstrom,R.J., Brown,M.P., Grillo,A., Roen,D. and Royer,C.A. (1997) Affinity and specificity of trp repressor-DNA interactions studied with fluorescent oligonucleotides. *J. Mol. Biol.*, **273**, 572–585.
- Boyer,M., Poujol,N., Margeat,E. and Royer,C.A. (2000) Quantitative characterization of the interaction between purified human estrogen receptor alpha and DNA using fluorescence anisotropy. *Nucleic Acids Res.*, **28**, 2494–2502.
- Senear,D.F., Ross,J.B. and Laue,T.M. (1998) Analysis of protein and DNA-mediated contributions to cooperative assembly of protein-DNA complexes. *Methods*, **16**, 3–20.
- Record,M.T., Jr, Zhang,W. and Anderson,C.F. (1998) Analysis of effects of salts and uncharged solutes on protein and nucleic acid equilibria and processes: a practical guide to recognizing and interpreting polyelectrolyte effects, Hofmeister effects and osmotic effects of salts. *Adv. Protein Chem.*, **51**, 281–353.

38. Khan, H., Buck, M. and Dixon, R. (1986) Deletion loop mutagenesis of the *nifL* promoter from *Klebsiella pneumoniae*: role of the -26 to -12 region in promoter function. *Gene*, **45**, 281–288.
39. Strauss, H.S., Burgess, R.R. and Record, M.T., Jr (1980) Binding of *Escherichia coli* ribonucleic acid polymerase holoenzyme to a bacteriophage T7 promoter-containing fragment: evaluation of promoter binding constants as a function of solution conditions. *Biochemistry*, **19**, 3504–3515.
40. Shaner, S.L., Melancon, P., Lee, K.S., Burgess, R.R. and Record, M.T., Jr (1983) Ion effects on the aggregation and DNA-binding reactions of *Escherichia coli* RNA polymerase. *Cold Spring Harb. Symp. Quant. Biol.*, **47**, 463–472.
41. Kao-Huang, Y., Revzin, A., Butler, A.P., O'Conner, P., Noble, D.W. and von Hippel, P.H. (1977) Nonspecific DNA binding of genome-regulating proteins as a biological control mechanism: measurement of DNA-bound *Escherichia coli* lac repressor *in vivo*. *Proc. Natl Acad. Sci. USA*, **74**, 4228–4232.
42. Cayley, S., Lewis, B.A., Guttman, H.J. and Record, M.T., Jr (1991) Characterization of the cytoplasm of *Escherichia coli* K-12 as a function of external osmolarity. Implications for protein-DNA interactions *in vivo*. *J. Mol. Biol.*, **222**, 281–300.
43. Schlax, P.J., Capp, M.W. and Record, M.T., Jr (1995) Inhibition of transcription initiation by lac repressor. *J. Mol. Biol.*, **245**, 331–350.
44. Popham, D.L., Szeto, D., Keener, J. and Kustu, S. (1989) Function of a bacterial activator protein that binds to transcriptional enhancers. *Science*, **243**, 629–635.
45. Tintut, Y., Wong, C., Jiang, Y., Hsieh, M. and Gralla, J.D. (1994) RNA polymerase binding using a strongly acidic hydrophobic-repeat region of σ^{54} . *Proc. Natl Acad. Sci. USA*, **91**, 2120–2124.
46. Record, M.T., Jr, Lohman, M.L. and De Haseth, P. (1976) Ion effects on ligand-nucleic acid interactions. *J. Mol. Biol.*, **107**, 145–158.
47. Lohman, T.M. and Mascotti, D.P. (1992) Thermodynamics of ligand-nucleic acid interactions. *Methods Enzymol.*, **212**, 400–425.
48. Schulz, A., Langowski, J. and Rippe, K. (2000) The effect of the DNA conformation on the rate of NtrC activated transcription of *E. coli* RNA polymerase σ^{54} holoenzyme. *J. Mol. Biol.*, **300**, 709–725.
49. Santero, E., Hoover, T.R., North, A.K., Berger, D.K., Porter, S.C. and Kustu, S. (1992) Role of integration host factor in stimulating transcription from the σ^{54} -dependent *nifH* promoter. *J. Mol. Biol.*, **227**, 602–620.
50. Cheema, A.K., Choudhury, N.R. and Das, H.K. (1999) A- and T-tract-mediated intrinsic curvature in native DNA between the binding site of the upstream activator NtrC and the *nifLA* promoter of *Klebsiella pneumoniae* facilitates transcription. *J. Bacteriol.*, **181**, 5296–5302.
51. Molina-López, J.A., Govantes, F. and Santero, E. (1994) Geometry of the process of transcription activation at the σ^{54} -dependent *nifH* promoter of *Klebsiella pneumoniae*. *J. Biol. Chem.*, **269**, 25419–25425.